A Message from the New Editor

It is an honour and a pleasure to take on the responsibility of the Editorship of THE MESSENGER. The former editors, and in particular Richard West who was editor for two terms (1976–1979 and 1986–1993), made the Messenger an informative and friendly publication. It is therefore clear that no large changes should be brought to the Messenger.

However, because of the forthcoming deployment of the VLT-VLTI, the ESO observers' community has an increasing need for technical information in all domains: site infrastructure, telescopes, instrumentation and detectors, calibration, data analysis and archiving. More emphasis will be given to these topics concerning both Paranal and La Silla. The Messenger will also carry articles on the use of the VLT-VLTI for specific astronomical topics. These articles are written by astronomers invited by the Editor to present their views. As before, observational results obtained at La Silla will also be presented. In this area, there will be no attempt at presenting a complete panorama of the observations carried out at ESO, and the number of articles in the observations section is likely to fluctuate from issue to issue. The most apparent change in the look of the journal is a division into sections: first the telescopes and instrumentation including detectors. This will be followed by articles on science with the VLT. Then there will be a section on scientific results obtained at La Silla and a section on other astronomical news. The last section groups all the announcements of ESO conferences and workshops, some announcements for positions (mostly in the Science Division), the titles of the accepted programmes and similar matters.

The technical editor of the Messenger remains Kurt Kjär and I look forward to our collaboration in producing the Messenger.

Marie-Hélène Ulrich
email Internet: mulrich@eso.org

TELESCOPES AND INSTRUMENTATION

The 8.2-m Primary Mirrors of the VLT

R. MUELLER, H. HOENESS, Schott Glaswerke, Mainz, Germany
J. ESPIARD, J. PASERI, REOSC, Longjumeau, France
P. DIERICKX, ESO

1. Introduction

The 8.2-m Zerodur primary mirrors of the VLT telescopes are on their way to the observatory. On June 25, the first of the four mirror blanks (code name Joe Dalton) was delivered by SCHOTT, the mirror blank manufacturer, to REOSC, who will polish it and mount its interfaces. Inspections performed before delivery have not only demonstrated the compliance of the blank with its specifications, but also the performance of the blank manufacturer in achieving superb quality.

On July 19 at 14:20, Joe was transported to Mainz harbour, a few kilometres away from the SCHOTT plant (Figure 1). At 9 p.m. it was loaded onto the barge ELDOR. The ELDOR went down the Rhine to Rotterdam, travelled south

to Calais, then up the Seine to Evry after crossing Paris on Friday 23 overnight. On Monday 26 at 10 a.m. it was unloaded and placed onto a trailer. The road transport to the REOSC plant started at 0:00 on Tuesday 27 and Joe arrived at REOSC at 02:30 a.m. The container was opened the same day at 14:00[1].

One of the greatest difficulties in the design of telescopes larger than about 4 or 5 metres is the manufacturing of the primary mirror blank. The classical design of a thick and solid mirror would imply enormous masses. First of a long series of problems, the homogeneity of a 200-ton casting is very unlikely to satisfy the stringent requirements applied to high accuracy optical components. Even under the unrealistic assumption that all manufacturing and assembling issues could be solved, an 8-m mirror more than 1 m thick would still deform too much under its own weight. Remember the basic idea: get a surface the size of a small appartment down to sub-micron accuracy, and maintain it.

There are three possible diets to get the mass down: reduce its weight, make it out of segments, or get it slim and use its support to control its shape. The three names behind these solutions are: Palomar, Keck, NTT, respectively. However, in the 8-m range, a Palomar-type primary mirror still needs some active control as gravity and thermal loads may affect the surface accuracy. The effectiveness (with regard to performance and safety) of very large honeycomb structures is still to be proven, while the second 10-m Keck telescope is on its way, and the NTT has already provided superb images. Each of the three solutions has its pros and cons, and the trade-off is extremely difficult. There are no miracles, just tremendous efforts to bring the concepts into operation.

2. The Actively Controlled Meniscus Concept

The concept selected by ESO for the VLT is an extrapolation of the concept demonstrated first with an experimental mirror 1 m in diameter and subsequently with the NTT. It consists of a f/1.8, 8.2-m diameter actively supported Zerodur meniscus, 175 mm thick. The mirrors will be supported axially by 150 hydraulic actuators. These actuators can be seen as computer-controlled springs: they do not constrain the spa-

Figure 1: *Joe on its way to Mainz harbour.*

tial position of the mirror at 150 locations but aim at providing a force distribution which results in a fully predictable elastic deformation of the mirror. With an active mirror, flexibility is used to compensate for manufacturing error and for on-line, real-time optimization of the optical properties of the telescope.

The hydraulic support system is divided into three sectors, each of them providing a virtual fixed point. Therefore, the axial position and tilt of the mirror is fixed. The actuators interface to the mirror through axial pads, the geometry of which is a three-leg spider. Each leg is connected to an invar pad about 50 mm in diameter, which is glued onto the convex surface. The distribution of the supports has been optimized to provide the lowest possible print-through on the mirror's surface. Additionally, the tripods introduce shear forces which reduce local deformations. The residual error is in the $\lambda/40$ rms range, and will be almost totally polished off as the mirrors are figured on their tripods. (See section 4.3, Effectiveness of the FLIP method.)

During operation the exact shape of the mirror will be monitored by Shack-Hartmann sensors. These sensors collect the light of an off-axis star to form an image of the pupil of the telescope onto a grid of lenses. A CCD camera records the distribution of the point images provided by the individual microlenses. A phase error of the incoming wavefront would imply a variable inclination of the rays with respect to the axis of each microlens thus resulting in a deviation from the nominal distribution

of spot images on the CCD. This deviation is measured and the wavefront reconstructed. The necessary correction is translated into a force distribution which is applied to the mirror through its active support. With active optics the frequency of correction is below about 1 Hz. With its six rings of support the VLT should be able to compensate errors with spatial frequencies up to about 1 m^{-1}, within an accuracy in the range of 50 to 100 nm rms, i.e. well beyond the effect of atmospheric turbulence.

On the user's side active optics should be fully automatic, i.e. the only noticeable effect should be the high quality of the data collected under permanent computerized optimization. Of course this situation is quite demanding in terms of tuning and reliability, and the concept inevitably requires permanent maintenance, as any large and complex telescope. On the other side the positive aspects of the active optics concept extend far beyond the potential excellence of the optical properties. Indeed it provides far more design and manufacturing perspectives than a passive concept, with positive consequences both on performance and cost.

The fragility of the thin meniscus requires particular attention. All supports and auxiliary equipment which will interface to the mirror at one stage or the other are designed to keep the probability of damage under about 10^{-5} under maximum loads. Nevertheless, given the high flexibility of the mirrors and the highly non-linear relation between damage probability and load parameters

(e.g. area of stress fields, magnitude of stress, duration, surface finish), transport, handling and operation of any large mirror have to follow strict and rigorous rules.

The mirror itself is made out of a highly homogeneous Zerodur substrate, with near-zero residual stresses. Table 1 summarizes the main specifications for the mirror blanks, together with the achievement by SCHOTT for the first mirror blank. In many respects the mirror blank is of exceptional quality.

In addition to the geometrical and material properties, the internal quality was specified in terms of maximum number of bubbles and inclusions. Again, the result is well within the specification. The convex surface has two holes (to be compared to 10 allowed), maximum diameter 34.8 mm and maximum depth 40 mm, which result from the removal of inclusions before ceramization. Local acid etching has been applied and the effect of the holes on stress fields is such that the probability of breakage is still beyond 10^{-5}.

The optical specifications given to the optical manufacturer are in line with the active optics concept and follow the formalism developed at ESO to quantify optical performance of ground-based telescopes.

The mirrors will be polished on an active support system which interfaces to the tripods. The manufacturer is permitted to physically remove low spatial frequency errors, provided that he stays within the specified budget of ±120 Newton maximum active force. The operational performance of the mirrors is given by the residual errors after active correction. The latter have been

Table 1.

Parameter	Specifications	Achievement	
Outer diameter	8200 ± 2	8201.52	mm
Inner diameter	1000 ± 0.5	999.81	mm
Concentricity	≤ 1	0.01	mm
Thickness[1]	176 + 2 −0	177.9	mm
Radius of curvature (concave surface)	28975	28968[2]	mm
(convex surface)	28977	28979[3]	mm
Profile tolerance (concave surface)	2	0.12[4]	mm
(convex surface)	2	0.05[5]	mm
Residual stresses (tensile)	≤ 0.10	max. 0.07	MPa
(compressive)	≤ 0.60	max. 0.08	MPa
Coefficient of thermal expansion (mean value)	0 ± 0.15	-0.043	10^{-6} °K^{-1}
(homogeneity)	≤ 0.05	0.009	10^{-6} °K^{-1}

[1] Normal to convex surface, on a diameter of 8160 mm. – [2] Best fitting sphere. – [3] Best fitting sphere. – [4] Including the effect of the 7 mm error on the radius of curvature of the concave surface. – [5] Including the effect of the 2 mm error on the radius of curvature of the concex surface.

specified in such a way that after convolution with the atmospheric seeing their effect on the long-exposure image will be limited to a maximum decrease of 5% of the peak intensity in stellar images, in the visible and with a seeing angle of 0.4 arcseconds full width at half maximum. It can be easily shown that the specification ensures simultaneously seeing-limited angular resolution and high signal throughput and signal-to-noise ratio.

A positive consequence of the active optics concept is that it allows the manufacturer to concentrate on high spatial frequency errors, which have usually lower amplitude but much higher slopes and are therefore more detrimental to performance than the low spatial frequency ones. In other words, an active mirror is likely to be smoother than a passive one, and therefore to provide better contrast and signal-to-noise ratio.

The issue of matching is less critical as well, as the active support can handle a fairly large error of the conic constant. Although the option of a pentaprism test on the primary and secondary mirrors combination can still be ordered, the current strategy for the VLT is to have separate cross-checks performed on the primary and secondary mirrors. These are direct tests, i.e. they do not involve relay lenses which could introduce systematic errors, and they aim at ensuring that no significant matching error is left.

As for any optical component, optical testing is essential as it should ensure that the manufacturing tolerances are fulfilled, and as a proper measurement of the surface data (radius of curvature and conic constant) is requested for the calibration of the field aberrations. Indeed, the latter have to be deducted from the off-axis measurement by the wavefront sensors, in order that the active system applies the appropriate corrections.

3. Mirror Blanks

Large-diameter and medium-thickness menisci are economically manufactured by using the spin casting technique. This technique was specifically developed by SCHOTT in 1986–1987 for the production of mirror blanks of the 8-m class. Contrary to the conventional casting technique, spin casting is able to produce a meniscus which approaches the final shape of the mirror with only small oversizing, thus reduced mass. The meniscus shape is obtained by rotating the mold (which has a spherical bottom) while the glass is not yet solidified.

The spin casting technique has proven successful in the production of several raw blanks of the 8-m class.
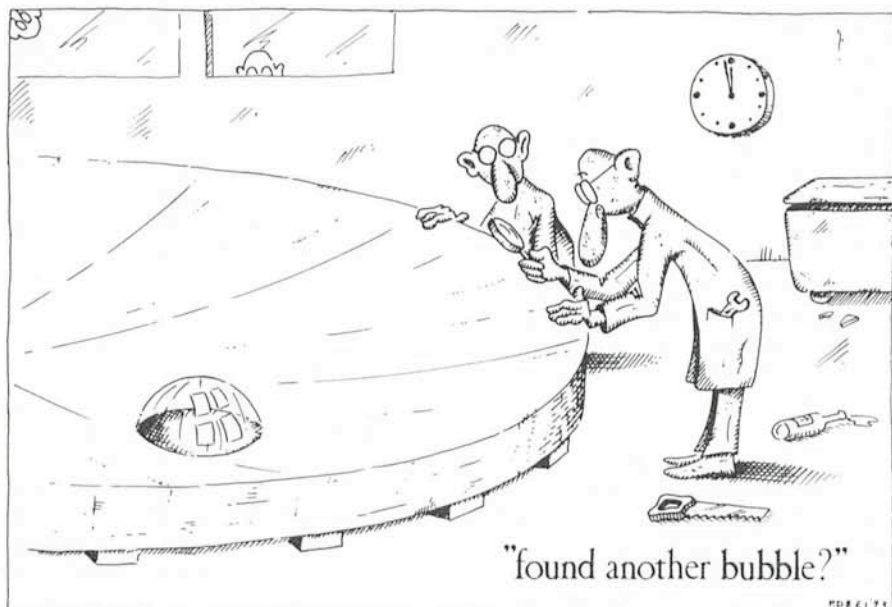

"found another bubble?"

Figure 2: *Lifting the overhead heating system.*

After the resolution of start-up problems, several castings could be successfully cooled down to room temperature. The subsequent quality inspections showed that the high requirements set to the inner quality of ZERODUR are completely fulfilled.

All subsequent operations like handling, ceramization and machining were carried out without any problems. The first blank is already delivered, and the second blank is currently in the process of being transformed into glass ceramics in the ceramization furnace.

For the spin casting production of mirror blanks of the 8-m class, all facilities and the respective buildings were built between June 1989 and March 1991. The facilities are entirely dedicated to the manufacture of ZERODUR blanks (mirror substrates of the 8-m class and smaller blanks of 0.6 m up to 4.4 m in diameter). Production structures include new buildings with about 50,000 m^3 of enclosed space, and modified and enlarged buildings.

The main steps of the manufacturing process are:

● Melting of glass in 70-t melting tank (discontinuous)

● Pouring of molten glass into the casting mold (which has a curved bottom), and generation of meniscus by spinning
● Coarse annealing of vitreous blank to ambient temperature
● Machining (rough grinding of front side, rear and edge)
● Transformation into glass ceramic (ceramization) by thermal retreatment
● Drilling of centre hole
● Final grinding

The handling and quality controls which are necessary between the individual production steps are not mentioned. In the following paragraphs the production process is described in some more detail.

● *Melting*

For this purpose, the batch is fed into the tank and melted, refined, and subsequently homogenized by stirring. A melting cycle lasts 24 days.

● *Pouring*

The casting mold is preheated for about 2 days, with the overhead heating system being lowered. Following this, the casting mold is lifted to allow the feeder (platinum tube for feeding the molten glass from the tank into the casting mold) to protrude downward from the bottom of the mold.

After heating the feeder nose with the help of proper devices, the molten glass flows from the melting tank onto a conveyer.

Then the mold is progressively lowered to keep the feeder nose at a specified distance of the bottom of the casting mold. The discharged glass flow is cut by an appropriate device which allows the casting mold to be filled while it is slowly being lowered. This filling operation lasts approximately 4 hours.

After completing the filling operation, the mold is moved from the casting area onto the spinning area with the help of the transfer vehicle.

● *Spinning*

Once the transfer vehicle has been fixed to the spinning unit along with the casting mold, the overhead heating system is fastened to and slightly lifted by some hoisting equipment from the casting mold (Figure 2). This is followed by spinning the casting mold containing the molten glass at a specified rotation rate. A cooling cap is placed above the mold after the concave upper surface of the glass has been produced. The released radiation energy (20 MW immediately after lifting the heating system) is dissipated through the evaporation of water. During the spinning phase, the molten glass cools down in such a way that the glass surface retains its contour. The spinning process lasts approximately 1 hour.

● *Annealing*

After the spinning process, the casting mold with the raw blank is entered into the annealing furnace. Subsequently, the transfer vehicle is moved out and the furnace is closed. This is followed by annealing the vitreous-state raw blank to ambient temperature. During this process, the blank is supported by an adaptable support system which follows the deformation and shrinking of the convex surface through the annealing process. The annealing period lasts approximately 3 months.

● *Lifting and turn-over*

When annealing has been completed, the annealing furnace is opened, after which the raw blank is lifted from the casting mold with a vacuum lifter and moved to the turning position by the crane equipment. There it is turned over (convex surface up) with the help of the turn-over installation (Figure 3).

Figure 3: *Turning the mirror blank.*

During all handling operations, deformations of the handling equipment should not be transferred to the blank. Therefore the handling equipment must have a flexible and adaptable coupling to the mirror blank. For this reason hydraulic cylinders are used. All support systems are designed in such a way that tensile stresses induced in the blank are kept well below 1 MPa.

● *Rough machining*

After turning over the raw blank, it is placed on the support system of the CNC grinding machine. This support system has a design similar to the design of the handling equipment. The blank convex surface and edge are roughly machined with diamond grinding wheels. This is followed by turning over the blank again and machining the front side.

● *Transformation to a semi-crystalline state (ceramization)*

After completing the rough machining the blank is submitted to a thermal after-treatment in the annealing furnace, which causes the vitreous state to be transformed into a semi-crystalline state. This procedure causes the material to acquire its outstanding properties of thermal *zero expansion*.

This crystallization process is exothermic. During crystallization, the volume shrinks by approximately 3%. Hence, all efforts should be made to cause crystallization to proceed very slowly, in order to prevent stresses from coming up and leading to the fracture of the disk due to non-controlled crystallization and resultant non-uniform shrinkage. This is why transformation from the vitreous to the semi-crystalline state takes approximately 8 months.

During the transformation process, the blank is supported by an adaptable support system within the annealing furnace.

● *Drilling of the centre hole and final grinding*

After transformation into a glass

Figure 4: *The blank during quality inspection.*

ceramic, the centre hole is drilled with the CNC grinding machine.

The final grinding is also performed on the machine, the accuracy of which is as follows:

Rotating table at 7000 mm diameter:

radial (x) runout	$< 10\ \mu m$
axial (z) runout	$< 15\ \mu m$
angular positioning	$< 120\ \mu m$

Positioning in x and z: $< 20\ \mu m$
Reproducibility in X and Z $< 2\ \mu m$

To preserve this accuracy the machine room has a temperature control giving

spatial temperature homogeneity
$< \pm 1.5°C$

temporal temperature inertia
$< \pm 1.5°C/h.$

● Quality controls

Quality controls and acceptance by customers are provided during and between the individual production steps (Figure 4).

Material characteristics are determined by the corporate Service RESEARCH & DEVELOPMENT. The project-tied inspection means consist of: overall geometric testing system (theodolite with process control computer), local geometric testing system, ultrasonic thickness gauge system, stress measuring system, video system for testing and documenting the inner quality. For stress measurements the blank is put onto a special quality control support system that generates extremely low stresses in the blank.

● Transfer to transportation system

After final acceptance, the blank is placed onto the transportation system with the vacuum lifter and the crane. The transportation system (REOSC) is assembled beforehand in the production wing.

4. Mirror Figuring and Polishing

On July 25, 1989, REOSC obtained from ESO the contract for the polishing of the four VLT mirrors and the following tasks:

● design and manufacture of the mirror handling tool and container,
● transportation of each VLT mirror blank from SCHOTT's plant in Mainz (Germany) to REOSC's plant,
● design, manufacture and assembly on the mirror of special devices for the mirror fixation in the cell,
● grinding, polishing and testing of the four VLT mirrors.

One of the governing design drivers in this project was the very important flexibility of the VLT mirrors as they feature a huge diameter of 8.2 m associated to a very low thickness of only 17.5 cm.

Figure 5: *The REOSC optical shop.*

4.1 THE OPTICAL SHOP

The new 8-m REOSC shop (Figure 5) was dedicated by the French Minister of Research and Space on April 24, 1992.

This plant is located close to the Seine, in order to optimize the mirror transport. Its total surface is 1100 m² and its dimensions are: length 70 m, width at the tower base 22 m, width of the shop 12.6 m, testing tower height 32 m.

4.2 OVERVIEW ON THE TECHNICAL PROCESS FOR FIGURING THE VLT MIRRORS

Due to their huge size and high flexibility, the conventional technique of the full sized flexible tool previously used for polishing and figuring has been modified in order to obtain a mirror surface free of high frequency defects and compliant with the requested aspherical shape.

Thus, the VLT mirrors will be ground and polished by using tools of adequate sizes associated with the REOSC Computer Controlled Surfacing (CCS) Process, and axially sustained by a support which is accurate enough not to blur the mirror high frequency defects with a large amount of non-axisymmetric low frequency defects.

Grinding machine

The grinding machine is composed of a rotating table, a removable milling bridge, a couple of two-arm machines designed and manufactured according to the REOSC requirements and a simplified axial support composed of 150 pneumatic actuators.

All this assembly is computer controlled through a unique console.

Polishing machine

The polishing machine (Figure 6) is identical to the grinding one but it is not permanently equipped with the milling bridge. Furthermore, this machine, located just under the testing tower, is equipped with an axial support of 150 pneumatic actuators, each of them is computer controlled through a Shack Hartmann CCD camera. The force accuracy delivered by each actuator is better than 2N and this support will be able to remove physically a large amount of low frequency defects.

The suppport software enables the user to adjust automatically the mirror position and its trim thanks to three length sensors. This software features also the mirror weighting, forces excerted by each actuator, mirror position, etc....

4.3 OVERVIEW OF THE TESTING METHODS

The testing facilities: the tower

As the efficiency of the optical tests depends on the vibration level, thermal stability and on the easiness to pass from a polishing run to a testing one, REOSC has given particular care in designing the testing tower which features an external sun shield, a main wall made of boarding with a thick lagging, an internal tower totally independent from the external one, made of a welded metallic structure which bears a double walled plastic tent. Thermally controlled air is inflected between the two walls of this tent.

Furthermore, in the testing tower, REOSC has foreseen the possibility to test the matching of a convex mirror associated with a concave mirror by using the Pentaprism method as already performed for the ESO 3.6-m telescope.

The testing plan

During the whole surfacing process of the VLT mirrors, the progress of the work is checked by the testing methods summarized in Table 2.

The mirror aspherical shape will be generated on the mirror at the rough grinding stage and checked by spherometry. Then the mirror will be moved to the polishing machine located under the tower. During the fine grinding, the mirror surface is tested by IR interferometry. When the mirror surface is smooth enough and about a few microns from the requested mirror shape, the polishing and the visible interferometric testing will start.

The spherometer

The spherometer body is made of an aluminium honeycomb structure. There are 8 points of measure and about 200 points of the mirror surface can be known. The estimated time for performing this measure and processing the data is about half an hour. The spherometer is carried by the milling bridge and its position and the position of the rotating table are controlled online by a computer to which are input the mirror sag measurements.

Visible interferometry and the Flow Interferogram Processing (FLIP)

The residual vibrations of the tower do not allow the use of the conventional phase shift method. The phase method based on Fourier transforms and the works of Claude and François Roddier lead to a too long processing time for averaging a large number of interferograms.

In order to overcome this difficulty, REOSC has developed a new algorithm which allows quick computing of the phase from only ONE interferogram which must present about 80 fringes inclined at 45° if a CCD camera of 250×250 pixels is used for an 8-m mirror. Furthermore, as an image can be
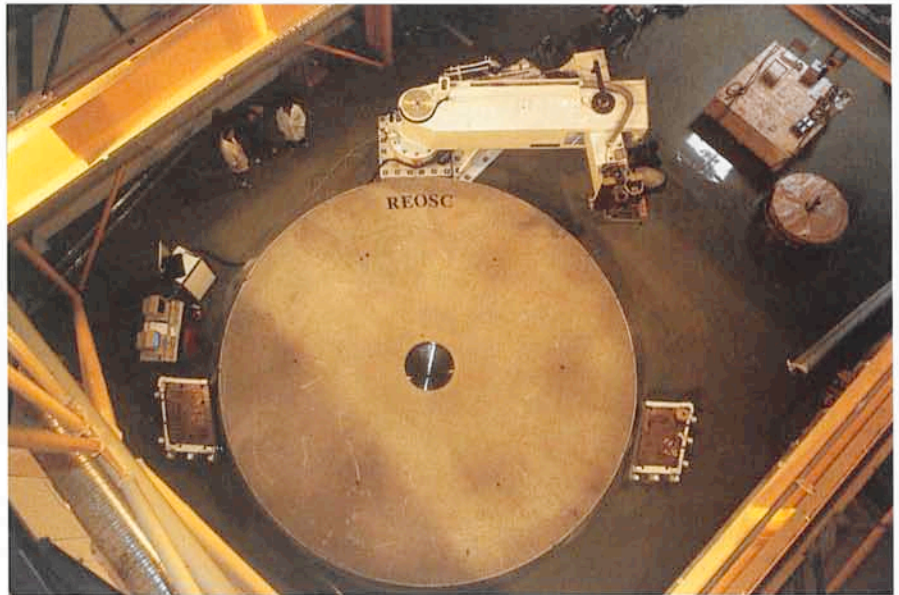

Figure 6: *The 8.2-m dummy mirror on the polishing machine, as seen from the test tower.*

caught in a thousandth of a second thanks to the use of an electronic shutter, the disturbing effect of the vibrations are eliminated.

FLIP is a special software which can be used with any interferometer provided it is equipped with a CCD camera and an electronic shutter. REOSC thinks that the FLIP method has the best money value.

The interferograms are taken by batches of 50 units and processed in 1 minute for 250×250 points with our present PC 386 equipped with a frame graber card, an accelerator card and a coprocessor. By adding two accelerator cards, the processing time can be divided by two. The residual vibrations of the tower combined with the averaging of the results allow the elimination of irregularities of illumination.

This software delivers the X and Y slope error map and the values of the RMS and P/V errors, the wavefront error map and the values of the RMS and P/V, as well as the mirror surface profile when the non-axisymmetric defects have been removed.

The programme is user friendly and it is now currently used in REOSC's optical shop.

Effectiveness of the FLIP method

In order to test the effectiveness of the VLT axial support when it is provided

with special tripods as interface between the actuator shaft head and the mirror, REOSC has figured a Zerodur spherical mirror of 1.7 m in diameter, 17.5 cm thick and with a radius of curvature of 28.8 m, the same as the VLT one. This mirror is in fact a part of a whole VLT mirror. For the experiment, this test mirror was resting on seven VLT actuators, each of them was provided with a tripod. Furthermore, some of them were equipped with a large dish in order to compare the residual high frequency defects between two kinds of support for polishing: on the tripod and on the dishes.

Since the testing tower of the new plant was not available at the date of this experiment, the 1.7-m mirror and its support were installed under the REOSC old testing tower of the 4-m mirror shop. The light beam was folded twice. The results obtained with this setup and the FLIP method are the following:

When the mirror is resting on 7 single points, the measured and computed mirror deformations are as shown in Table 3.

There is a perfect correlation between the experiment and the FE computation.

In order to evaluate the FLIP ability to detect minute defects among larger ones, we have compared the results obtained by finite elements computation and FLIP measurements when the mirror is resting on the tripods.

The mirror figure obtained by interferometry is the averaging of a batch of 50 interferograms taken by the FLIP method to which we have substracted the 1.7-m mirror figure (see Table 4).

The conclusion is that the finite elements results are very close to the experimental ones. The difference in the

Table 2.

Manufacturing stage	Test	Number of points	Absolute accuracy	Sensitiveness P/V	Tower requested
Rough grinding	Spherometry	198	5000 nm	1000 nm	No
Fine grinding	IR Interferometry	2000	500 nm	300 nm	Yes
Polishing, final figuring	FLIP method	250×250	5 nm	5 nm	Yes

Table 3.

	Interferometry		Computation	
	P/V	RMS	P/V	RMS
Mirror surface	148 nm	24 nm	107 nm	25 nm

P/V values comes from the presence in the laser beam of some artefacts which generate a few local sharp defects.

It is worth noting that the RMS value of the high frequency defects generated by the axial support is three times lower when the mirror is resting on the tripods. This factor of three is in very good agreement with the computation.

In order to evaluate the noise of the measurements, we have computed the difference between the average of three batches of fifty interferograms of the mirror resting on the tripods. The RMS error on the mirror surface error is 5.6 nm.

Table 4.

	Interferometry		Computation	
	P/V	RMS	P/V	RMS
Mirror surface	59 nm	7.3 nm	37 nm	8 nm

5. Conclusion

Joe Dalton was delivered in time and well within specifications. It is now lying on the grinding machine at REOSC, where everything is ready for the next steps: glueing of the axial interfaces (in August 1993), followed by the exciting tasks of grinding it aspherical to a few microns accuracy, and then polishing to optical accuracy. Looking forward to meeting Bill, William and Averell!

Ground-Based Astronomy in the 10 and 20 μm Atmospheric Windows at ESO – Scientific Potential at Present and in the Future

H. U. KÄUFL, ESO

1. Introduction

This article is especially written for those who have little or no experience with astronomical observations in the infrared, especially longwards of 2.2 μm. In recent issues of the *Messenger* (Käufl et al. 1992, Käufl 1993) there were several reports on instrumentation at ESO for observations in the 10 and 20 μm atmospheric windows (N and Q band in Johnson's photometric system). In this article a description of the perspectives of ground-based astronomy in these windows will be given. A special focus is set on the astronomical applications with respect to what is possible (and what not) with the present equipment; which improvements are anticipated at the VLT and how these observations compare to air-borne and space-based infrared astronomy.

2. Targets for Ground-based Infrared Observations at Wavelengths longer than 5 μm[1]

2.1 Atmospheric constraints

The terrestrial atmosphere has a substantial opacity in the infrared due to

---

[1] Some of the argumentation holds also for the range of 3–5 μm. This transition region between the near infrared and the thermal infrared, however, is outside the scope of this article.

rotational-vibrational transitions of trace molecules (e.g. CO_2, H_2O, CH_4, O_3). In some spectral regions these molecular transitions blend creating a practically opaque sky. The region between 8 and 13 μm, however, is reasonably free of interfering molecular transitions. Remaining absorption lines in the window itself and at the "red" edge are rather stable and observations can be easily corrected for these perturbations. On the "blue" edge H_2O is a source of variable opacity following the rapid variations of local humidity. Close to this edge more careful observing procedures are required. Beyond ≈ 13.3 μm the atmosphere becomes opaque due to the ν_2-band of CO_2 and opens again around 16.5 μm. A forest of lines of H_2O, however, prevents the sky from getting clear so that even in the best part of the 20 μm window the average opacity more or less corresponds to 50 % and is variable. Beyond 20 μm the water vapour lines become a real problem. The term "Q-window" is misleading and should be replaced by "Q-venetian-blind". Depending on site and local weather, limited astronomical observations are possible up to 30-35 μm. Beyond ≈ 35 μm the atmosphere remains opaque until the sub-millimetre region (≥ 300 μm) is reached.

In conclusion, long wavelength in-frared astronomical observations are constrained to:

- $\lambda \approx 8$–13 μm with very good conditions
- $\lambda \approx 16.5$–30 μm with reasonable to poor conditions

2.2 Wien's Law, Kirchhoff's Law and their consequences

Wien's law relates the maximum of the Planck curve for black body radiation with its temperature

$$\lambda_{max} = \frac{2898 \, \mu m}{T[K]}$$

For a telescope at ambient temperature λ_{max} lies exactly in the centre of the 10 μm atmospheric window. Translated into the words of optical astronomy this is equivalent to observing stars from within a furnace (like the one in which the VLT blanks have been casted) rather than from a dark astronomical site.

To those readers not familiar with infrared astronomy it is also useful to recall Kirchhoff's law

$$\alpha(\lambda, T) = \varepsilon(\lambda, T)$$

which states that for all wavelengths and temperatures the emissivity equals exactly the absorptivity. For ground-based infrared astronomy this means that e.g. a